

Molecular Traffic Control in Porous Nanoparticles

Andreas Brzank^{1,2*} and Gunter Schütz¹

¹*Institut für Festkörperforschung, Forschungszentrum Jülich, 52425 Jülich, Germany*

²*Fakultät für Physik und Geowissenschaften,
Universität Leipzig, Abteilung Grenzflächenphysik,
Linnestrasse 5, D-04103 Leipzig, Germany*

(Dated: November 8, 2018)

Abstract

We investigate the conditions for reactivity enhancement of catalytic processes in porous solids by use of molecular traffic control (MTC) as a function of reaction rate and grain size. With dynamic Monte-Carlo simulations and continuous-time random walk theory applied to the low concentration regime we obtain a quantitative description of the MTC effect for a network of intersecting single-file channels in a wide range of grain parameters and for optimal external operating conditions. The efficiency ratio (compared with a topologically and structurally similar reference system without MTC) is inversely proportional to the grain diameter. However, for small grains MTC leads to a reactivity enhancement of up to approximately 30% of the catalytic conversion $A \rightarrow B$ even for short intersecting channels. This suggests that MTC may significantly enhance the efficiency of a catalytic process for small porous nanoparticles with a suitably chosen binary channel topology.

*Electronic address: a.brzank@fz-juelich.de

I. INTRODUCTION

Zeolites are used for catalytic processes in a variety of applications, e.g. cracking of large hydrocarbon molecules. In a number of zeolites diffusive transport occurs along quasi-one-dimensional channels which do not allow guest molecules to pass each other [1]. Due to mutual blockage of reactand A and product molecules B under such *single-file conditions* [2] the effective reactivity of a catalytic process $A \rightarrow B$ – determined by the residence time of molecules in the zeolite – may be considerably reduced as compared to the reactivity in the absence of single-file behaviour. It has been suggested that the single-file effect may be circumvented by the so far controversial concept of molecular traffic control (MTC) [3, 4]. This notion rests on the assumption that reactands and product molecules resp. may prefer spatially separated diffusion pathways and thus avoid mutual suppression of self-diffusion inside the grain channels.

The necessary (but not sufficient) requirement for the MTC effect, a channel selectivity of two different species of molecules, has been verified by means of molecular dynamic (MD) simulations of two-component mixtures in the zeolite ZSM-5 [5] and relaxation simulations of a mixture of differently sized molecules (Xe and SF₆) in a bimodal structure possessing dual-sized pores (Boggsite with 10-ring and 12-ring pores) [6]. Also equilibrium Monte-Carlo simulations demonstrate that the residence probability in different areas of the intracrystalline pore space may be notably different for the two components of a binary mixture [7] and thus provide further support for the notion of channel selectivity in suitable bimodal channel topologies.

Whether a MTC effect leading to reactivity enhancement actually takes place was addressed by a series of dynamic Monte Carlo simulations (DMCS) of a stochastic model system with a network of perpendicular sets of bimodal intersecting channels and with catalytic sites located at the intersecting pores (NBK model) [9, 10, 11]. The authors of these studies found numerically the occurrence of the MTC effect by comparing the outflow of reaction products in the MTC system with the outflow from a reference system with equal internal and external system parameters, but no channel selectivity (Fig. 1). The dependency of the MTC effect as a function of the system size has been investigated in [12]. The MTC effect is favored by a small number of channels and occurs only for long channels between intersections, which by themselves lead to a very low absolute outflow compared to a

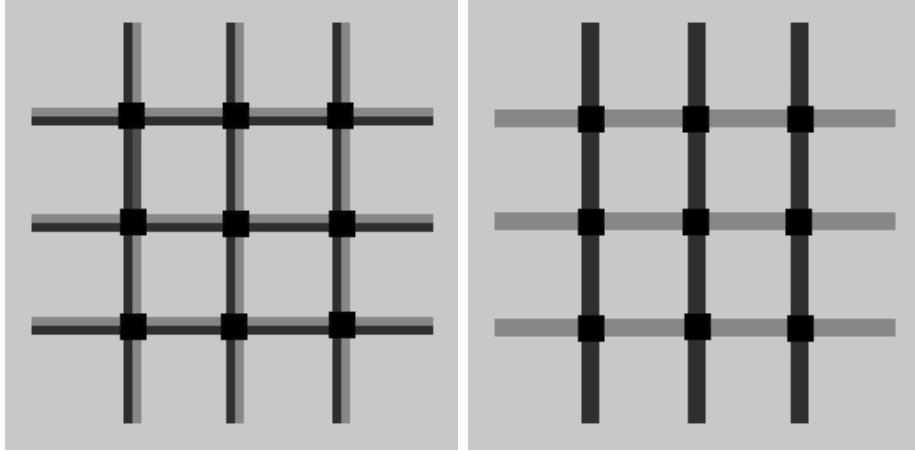


FIG. 1: REF system (left) with $N = 3$ channels and MTC system (right) of the the same size. In contrast to the REF case, where we allow both types of particles (A and B particles) to enter any channel, in the MTC system A particles are carried through the vertical α channels whereas the B particles diffuse along the horizontal β channels. Black squares indicate catalytic sites where a catalytic transformation $A \rightarrow B$ is allowed.

similar system with shorter channels. A recent analytical treatment of the master equation for this stochastic many-particle model revealed the origin of this effect at high reactivities [13]. It results from an interplay of the long residence time of guest molecules under single-file conditions with a saturation effect that leads to a depletion of the bulk of the crystallite. Thus the MTC effect is firmly established, but the question of its relevance for applications remains open.

Here we address this question by a systematic study of the MTC effect as a function of the reactivity of the catalytic sites and as a function of grain size, but using fixed small channel length. This choice is motivated by potential relevance from an applied perspective. Moreover, for the same reason we determine the MTC effect by making a comparison with the reference system using the same set of fixed internal (material-dependent) parameters, but (unlike in previous studies [11, 12, 13]) for each case (MTC and REF resp.) different optimal external (operation-dependent) parameters which one would try to implement in an industrially relevant process. It will transpire that a significant MTC effect (reactivity enhancement up to $\approx 30\%$) occurs in our model system even for small channel length at realistic intermediate reaction rates of the catalyst, provided the grain size is sufficiently small. This may be of interest as since the first successful synthesis of mesoporous MCM-41

nanoparticles [14], there has been intense research activity in the design and synthesis of structured mesoporous solids with a controlled pore size. In particular, synthesis of bimodal nanostructures with independently controlled small and large mesopore sizes has become feasible [15].

In this work we do not study a specific process in a specific material, but we demonstrate the validity of the MTC concept even if channels inside the porous material are short. This is novel and – from an applied viewpoint – crucial since it is a necessary condition for starting expensive and time-consuming quantitative investigations in specific settings.

II. NBK MODEL

As in [12, 13] we consider the NBK lattice model [9] with a quadratic array of $N \times N$ channels (Fig. 1) which is a measure of the grain size of the crystallite. Each channel has L sites between the intersection points where the irreversible catalytic process $A \rightarrow B$ takes place. We assume the boundary channels of the grain to be connected to the surrounding gas phase, modelled by reservoirs of constant densities such that the entrances of the respective channels (extra reservoir sites) have a fixed A particle density ρ . We assume the reaction products B which leave the crystallite to be removed immediately from the gas phase such that the density of B particles in the reservoir is always 0. Short-range interaction between particles inside the narrow pores is described by an idealized hard core repulsion which forbids double-occupancy of lattice sites.

The underlying dynamics are stochastic. We work in a continuous time description where the transition probabilities become transition rates and no multiple transitions occur at the same infinitesimal time unit. Each elementary transition between microscopic configurations of the system takes place randomly with an exponential waiting-time distribution. Diffusion is modelled by jump processes between neighbouring lattice sites. D is the elementary (attempt) rate of hopping and is assumed to be the same for both species A, B of particles. In the absence of other particles D is the self-diffusion coefficient for the mean-square displacement along a channel. If a neighboring site is occupied by a particle then a hopping attempt is rejected (single-file effect). The dynamics inside a channel are thus given by the symmetric exclusion process [16, 17, 18, 19] which is well-studied in the probabilistic [20] and statistical mechanics literature [21]. The self-diffusion along a channel is anomalous,

the effective diffusion rate between intersection points decays asymptotically as $1/L$, see [18] and references therein.

At the intersections the reaction $A \rightarrow B$ occurs with a reaction rate c . This reaction rate influences, but is distinct from, the effective grain reactivity which is largely determined by the residence time of guest molecules inside the grain which under single-file conditions grows in the reference system with the third power of the channel length L [22]. At the boundary sites particles jump into the reservoir with a rate $D(1 - \rho_A - \rho_B)$ in the general case. Correspondingly particles are injected into the grain with rates $D\rho_{A,B}$ respectively. As discussed above here we consider only $\rho_A = \rho$, $\rho_B = 0$.

For the REF system A and B particles are allowed to enter and leave both types of channels, the vertical (α) and horizontal (β) ones. In case of MTC $A(B)$ particles will enter $\alpha(\beta)$ -channels only, mimicking complete channel selectivity. Therefore all channel segments carry only one type of particles in the MTC case. For the boundary channels complete selectivity implies that α -channels are effectively described by connection with an A -reservoir of density $\rho_A = \rho$ (B -particles do not block the boundary sites of α -channels) and β -channels are effectively described by connection with a B -reservoir of density $\rho_B = 0$, respectively. (A -particles do not block the boundary sites of β -channels.) This stochastic dynamics, which is a Markov process, fully defines the NBK model.

In both cases, MTC and REF system, the external concentration gradient between A and B reservoir densities induces a particle current inside the grain which drives the system in a stationary nonequilibrium state. For this reason there is no Gibbs measure and equilibrium Monte-Carlo algorithms cannot be applied for determining steady state properties. Instead we use dynamic Monte-Carlo simulation (DMCS) with random sequential update. This ensures that the simulation algorithm yields the correct stationary distribution of the model.

III. MONTE CARLO RESULTS

Anticipating concentration gradients between intersection points we expect due to the exclusion dynamics linear density profiles within the channel segments [13, 17, 21], the slope and hence the current being inversely proportional to the number of lattice sites L . The total output current j of B particles, defined as the number of B -particles leaving the grain per time unit in the stationary state, is the main quantity of interest. It determines the

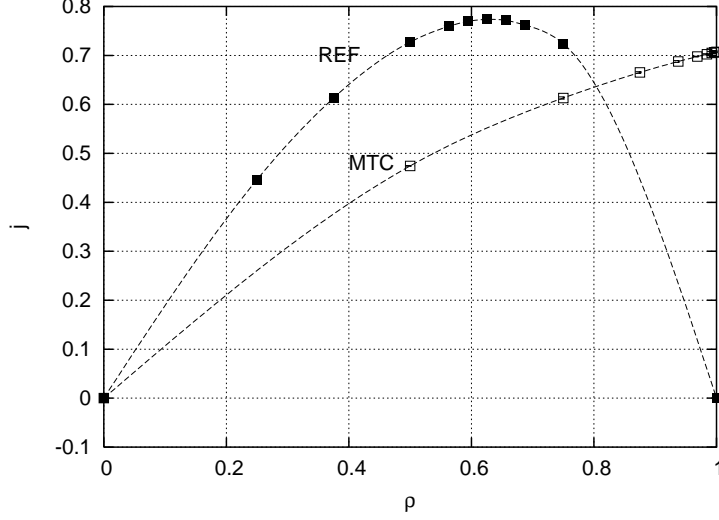


FIG. 2: j_{REF} (solid symbols) and j_{MTC} (open symbols) as a function of the reservoir density for a system with $N = 5$, $L = 1$, $c = 0.1$.

effective reactivity of the grain.

We are particularly interested in studying the system in its maximal current state for given reactivity c and size constants N , L , which are intrinsic material properties of a given grain. The A particle reservoir density ρ , determined by the density in the gas phase, can be tuned in a possible experimental setting. Let us therefore denote the reservoir density which maximizes the output current by ρ^* and the maximal current by j^* . For MTC systems as defined above we always expect $\rho_{MTC}^* = 1$, since the highly charged entrances of α -channels do not block the exit of B -particles and hence do not prevent them from leaving the system. Fig. 2 shows j as a function of ρ for both a MTC and REF system of $N = 5$, $L = 1$ and reactivity $c = 0.1$. Indeed for MTC the maximal output occurs for the maximal reservoir density. In case of the REF system ρ_{REF}^* as well as j_{REF}^* need to be found by simulation. We iteratively approach the maximal current by a set of 9 datapoints. The "best" datapoint has been chosen in order to approximate the maximum. Statistical errors are displayed. They are, however, mostly within symbol size.

In order to measure the efficiency of a MTC system over the associated REF system we define the efficiency ratio

$$R(c, N, L) = \frac{j_{MTC}^*}{j_{REF}^*} \quad (1)$$

which is a function of the system size N , L and reactivity c .

Fig. 3 (left) shows the measured ratio R for a large range of reactivities. We plotted

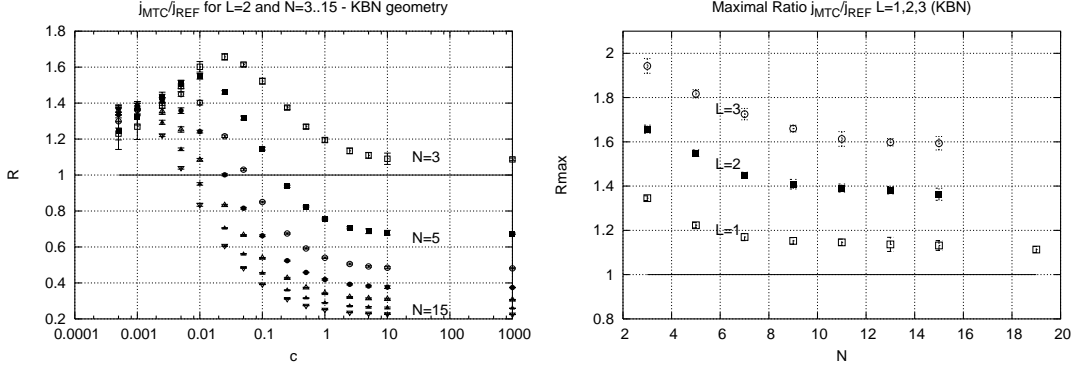


FIG. 3: Left: Ratio $R(c)$ for different number of channels N and $L = 2$. Right: Maximal ratio R^* for different L

systems with $L = 2$ and different N . We note that the MTC effect has a strong negative dependence on increasing N for all N and increasing c above some optimal value c^* . We denote this optimal value by R_{max} . Fig. 3 (right) shows $R_{max}^*(N)$ for different L and proves that there is an MTC effect for any L and any N . Notice, however, that with increasing N the optimal ratio not only decreases, but appears at unnaturally small reactivities c . This is highly undesirable as then the actual output current shrinks to zero. Even though more efficient than a REF system, a MTC grain with large N would not operate under practically relevant conditions.

As expected from previous results [12, 13] the MTC effect is seen to increase with increasing L , even though the measure R used here is different (Fig. 4). This follows from theoretical studies of single-file systems. The mean traveling time of a product molecule through a channel of length L is proportional to L^2 in the MTC case as in ordinary diffusion, but proportional to L^3 in the REF case due to mutual blockage. Hence the current is proportional to $1/L$ in a MTC system, but proportional to $1/L^2$ in a REF system. This holds for all values of the parameters and hence for sufficiently large L the MTC system becomes more efficient.

In order to understand the strong decrease of R for large reactivities and large number of channels it is instructive to study the stationary density profiles. Fig. 5 shows the B particle densities for a REF system (left) and MTC system (right) with $N = L = 9$ and large reactivity $c \rightarrow \infty$. Theoretical investigations of MTC systems in the large reactivity case [13] show that in the state of maximal current ($\rho = 1$) the output of B particles is independent of the number of channels. For large L the maximal output current becomes

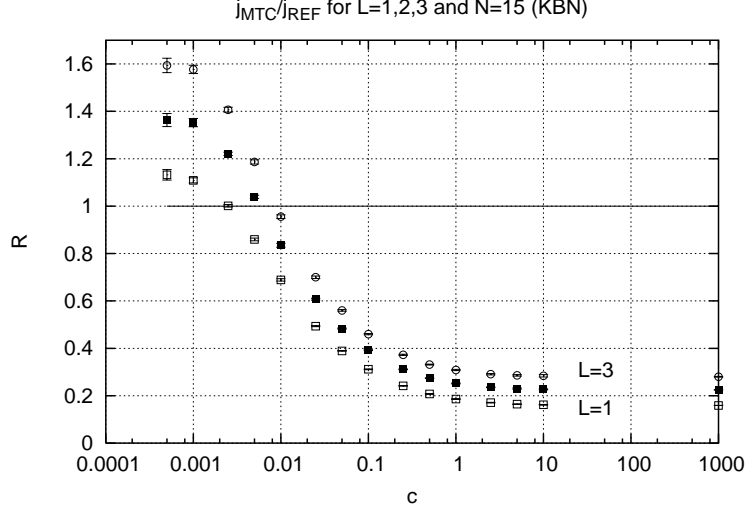


FIG. 4: Dependence of the output ratio on the channel length L .

$j_{c \rightarrow \infty}^* \simeq \frac{4D}{L}$ where D is the diffusion constant. A nonvanishing current of B particles can be observed only at the four corners of the lattice (Fig. 6 right).

For fixed moderate c this extreme situation is not realized, but nevertheless with increasing N one expects that the bulk gets increasingly depleted, since in each layer a fraction of A particles is converted into B particles. Thus the total A -density in each layer may be described by the form

$$\frac{d}{dx} N_A(x) = -\gamma N_A(x) \quad (2)$$

The coarse-grained ansatz for the number $N_A(x)$ of A -particles in layer x predicts an exponential decrease of the A density, leaving only an active boundary layer of finite thickness

$$\xi = 1/\gamma \propto 1/c \quad (3)$$

at the top and bottom respectively of the (in our simulation two-dimensional) grain. Hence, as a function of N , j_{MTC}^* saturates at some constant

$$\lim_{N \rightarrow \infty} j_{MTC}^*(c, N, L) = C_{MTC}^*(c, L). \quad (4)$$

On the other hand, in the REF system the output current scales linearly with increasing N for all, even large, c (Fig. 6 left). This is because even though again the bulk depletes with increasing N the active boundary layer is a surface scaling linearly with N . Thus

$$\lim_{N \rightarrow \infty} j_{REF}^*(c, N, L) = NC_{REF}^*(c, L) \quad (5)$$

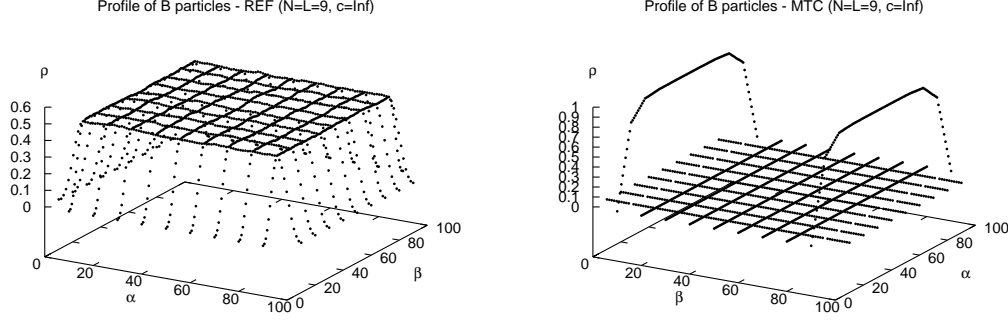


FIG. 5: Profiles of the REF (left) and MTC (right) system in the large-reactivity case. $N = L = 9$

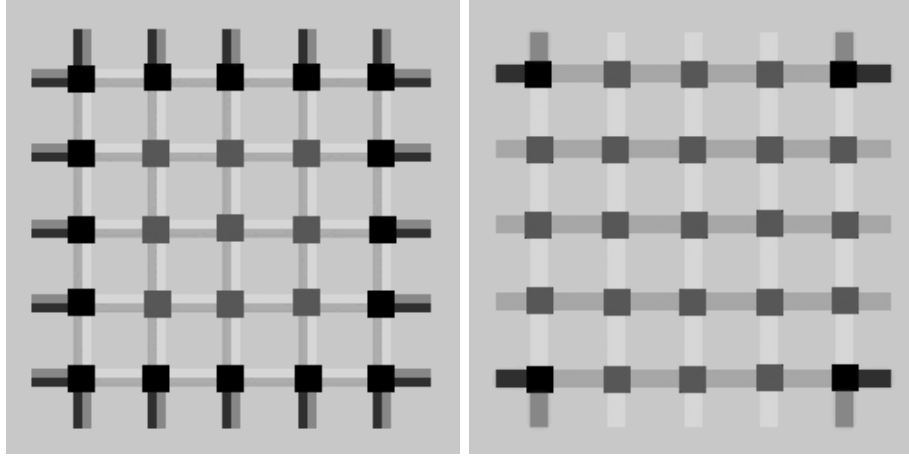


FIG. 6: Active channel segments in the large-reactivity case. REF system (left), MTC system (right)

Hence

$$R(c, N, L) \propto 1/N \quad (6)$$

and the MTC effect vanishes at some N for fixed reactivity c and channel length L .

Looking on a wider range of reactivities (Fig. 7) we notice that the maximal currents for MTC systems saturate for some intermediate c whereas in the REF case the current reaches a plateau for large reactivities. This observation can be rationalized by noticing that an increase of the output with increasing c is limited by the incoming current of available A particles. Since in the REF system A and B particles block each other an increasing current of B -particles always restricts the number of A particles diffusing in. Hence the saturation due to high reactivity sets in only for larger values of c than in the MTC system.

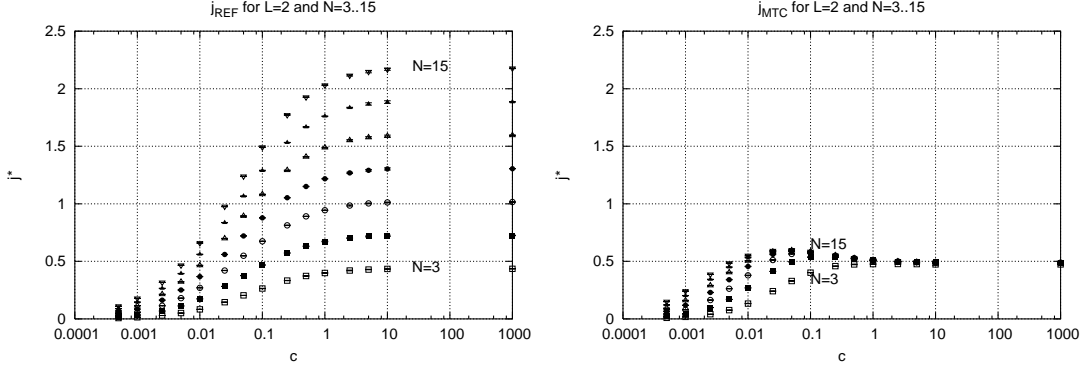


FIG. 7: Maximal currents for the REF system (left) and the MTC system (right). $L = 2$ and different N .

IV. REF WITH SMALL REACTIVITIES

The arguments put forward above for explaining qualitative and quantitative features of the MTC effect at intermediate and large reactivities c fail for small reactivities, i.e., when c is of the order of the inverse mean intracrystalline residence time. We first consider the reference system.

In this case the grain contains only a very small number of B particles at any time. In this low-concentration regime the diffusion of B particles inside the grain may be described by a linear diffusion equation with an effective diffusion coefficient determined by the interaction with A particles as follows. The A particles are considered as a medium with constant equilibrium density ρ throughout the system. At the intersections B particles are created randomly with effective rate $c\rho$. We then describe the diffusion of a B particle in the channel between intersections by a random walk from intersection to intersection with an effective diffusion constant D_{eff} given by the (inverse) mean travelling time between intersections. Let $\rho_{(x,y)}$ be the B particle density at the intersection denoted by (x,y) and Δ a discrete two-dimensional Laplace operator

$$\Delta\rho_{(x,y)} = \frac{1}{4} (\rho_{(x+1,y)} + \rho_{(x-1,y)} + \rho_{(x,y+1)} + \rho_{(x,y-1)} - 4\rho_{(x,y)}) . \quad (7)$$

Here the lattice unit is given by the channel length rather than the pore size inside a channel. For the B particle density at intersections we thus obtain

$$\frac{\partial}{\partial t}\rho_{(x,y)} = D_{eff}\Delta\rho_{(x,y)} + c\rho. \quad (8)$$

A stationary solution to (8) can be found by use of the discrete sine transform $\tilde{\rho}_{(q,p)} =$

$\sum_{x=1}^N \sum_{y=1}^N \rho_{(x,y)} \sin \frac{q\pi x}{N+1} \sin \frac{p\pi y}{N+1}$. We express (8) (with vanishing time derivative) in terms of the transformed density $\tilde{\rho}_{(q,p)}$. Taking into account the boundary conditions $\rho_{0,y} = \rho_{x,0} = \rho_{x,N+1} = \rho_{N+1,y} = 0$ with $0 \leq x, y \leq N+1$ we find

$$\tilde{\rho}_{(q,p)} = \frac{2c\rho_A}{\cos \frac{q\pi}{N+1} + \cos \frac{p\pi}{N+1} - 2} \sum_{n=1}^N \sum_{m=1}^N \sin \frac{q\pi n}{N+1} \sin \frac{p\pi m}{N+1}. \quad (9)$$

The non zero contributions of the double sum can be expressed as a product of two Cotangents. Transforming back finally yields

$$\rho_{(x,y)} = \lambda \sum_{n=1}^N \sum_{m=1}^N \frac{B_{(n,m)}}{\cos \frac{n\pi}{N+1} + \cos \frac{m\pi}{N+1} - 2} \sin \frac{n\pi x}{N+1} \sin \frac{m\pi y}{N+1} \quad (10)$$

$$B_{(n,m)} = \begin{cases} 0 & \text{if } n \text{ or } m \text{ even} \\ \frac{1}{(N+1)^2} \cot \frac{m\pi}{2(N+1)} \cot \frac{n\pi}{2(N+1)} & \text{else} \end{cases} \quad (11)$$

D_{eff} together with the reactivity and reservoir density, is absorbed into a fitting parameter $\lambda \sim \frac{c\rho}{D_{eff}}$. With $\rho_{(x,y)}^{Sim}$ being the B particle densities obtained from simulations and $\rho_{(x,y)}^{Th}$ the theoretical densities, we define the homogenized mean square deviation

$$Q := \frac{2}{N} \sqrt{\sum_{\text{intersections}} \left(\frac{\rho_{(x,y)}^{Sim} - \rho_{(x,y)}^{Th}}{\rho_{(x,y)}^{Sim} + \rho_{(x,y)}^{Th}} \right)^2} \quad (12)$$

as a measure for the quality of the approximation. The sum runs over all intersections, with the local deviation normalized by the local mean. This assures that all intersections contribute with their proper weight.

For large c the profile flattens (see Fig. 5) and is not very well described by (10). Fig. 8 shows Q as a function of c . The boundary density has been chosen to $\rho = 0.5$. For small reactivities the collapse of the simulated and calculated profile is fairly good ($Q \approx 0.1$). However, the best collapse occurs for small intermediate reactivities. This somewhat peculiar behavior can be explained by assuming that this random walk is not a Markov process as implied in the derivation of (10). The structural change in the occupation of the channel segment, once a particle covered the distance between two adjacent intersections, implies a "memory" effect. Hence we cannot assume perfect statistical independence of subsequent random traveling times between intersections which implies that the Markov assumption is not very well satisfied. As we increase the reactivity more than one B particle may be present in the system. This corresponds to an ensemble average over

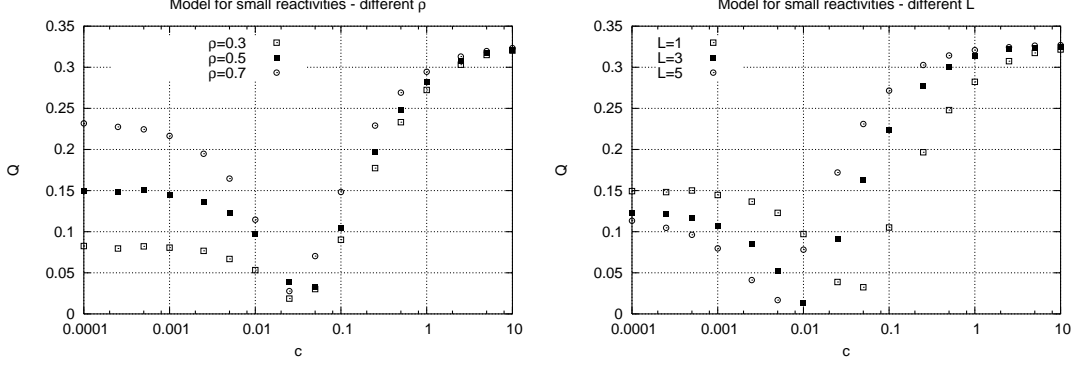


FIG. 8: Collapse of the simulated and calculated profiles for REF systems. Left: $N = 5$, $\rho = 0.5$ and different L . (right) $N = 5$, $L = 1$ and different ρ .

almost independent random walkers which cancels the time correlations of each individual walker and thus improves the validity of the Markov assumption. This leads to the good data collapse for some intermediate reactivities. As c increases further both the assumption of equilibrium of A particles and the low-concentration approximation (8) for B particles fail.

V. MTC WITH SMALL REACTIVITIES

Fig. 9 shows the stationary density profiles of a MTC system with small reactivity. We first note that the output current is proportional to the number N of β exit channels, in agreement with the observation that R_{max} approaches a constant for large N , rather than decaying proportional to $1/N$ as R for fixed reactivity does. Moreover, due to rare transition events all α -channels are almost in equilibrium with the reservoir (Fig. 9 left). Thus it is sufficient to single out only one β channel.

We adapt the approach we took for the REF system to the present case. Due to low concentration we use a linear diffusion equation for the B -density inside a β -channel. There are, however, two essential differences. (1) Because of the absence of A -particles we do not consider the occupation of intersections alone, but we track the motion of B particles inside a channel. (2) Due to the inequivalence of the sites inside the β -channels and the intersection points where also A may be located, we need to describe a random walker with space dependent hopping rates. Intersections, on the one hand, serve as sites of B particle creation with a rate proportional to the reactivity. On the other hand intersections are

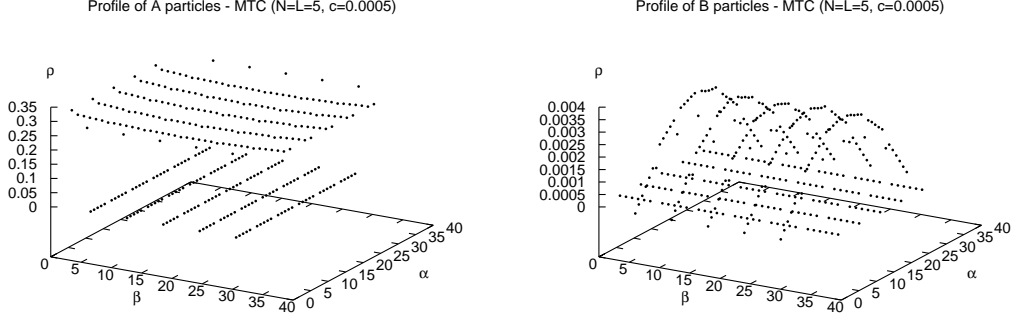


FIG. 9: Profiles for a MTC system $N = L = 5$ and small reactivity $c = 0.005$. (left) densities of A and (right) of B particles. $\rho = 0.3$

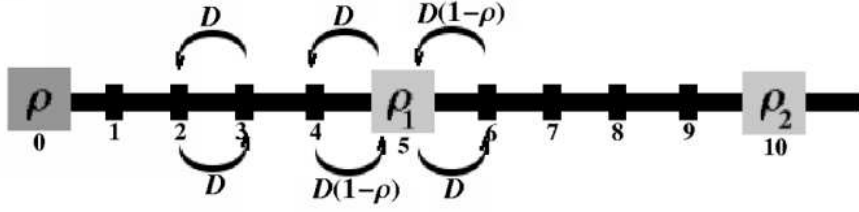


FIG. 10: β channel with hopping rates. $L = 4$

occupied by A particles with a probability ρ and hence, block B particles. This leads to different hopping rates onto and from an intersection as displayed in Fig. 10.

The master equation description leads to a set of equations for the local B particle densities $\langle n_x \rangle$.

$$\frac{d}{dt} \langle n_x \rangle = \begin{cases} D (\langle n_{x-1} \rangle + \langle n_{x+1} \rangle - \langle n_x \rangle - (1 - \rho) \langle n_x \rangle) & x = (L+1)r \pm 1 \\ D (1 - \rho) (\langle n_{x-1} \rangle + \langle n_{x+1} \rangle) - 2D \langle n_x \rangle + c\rho & x = (L+1)r \\ D (\langle n_{x-1} \rangle + \langle n_{x+1} \rangle - 2 \langle n_x \rangle) & \text{else} \end{cases} \quad (13)$$

Here x is the lattice position inside a channel in units of the pore size. In the stationary state left hand side of (13) vanishes and it follows a recurrence relation for the B-particle intersection densities $\rho_r \equiv \langle n_{(L+1)r} \rangle$.

$$\rho_r = \frac{1}{2} (\rho_{r+1} + \rho_{r-1} + K) \quad (14)$$

$$K = \frac{c\rho}{D} [(L+1) - (L-1)\rho] \quad (15)$$

The inhomogeneity K depends on the segment length L and the transition rates. A solution satisfying (14) and the boundary condition $\rho_0 = \rho_{N+1} = 0$ can be obtained by use of a quadratic ansatz. We find

$$\rho_r \equiv \langle n_{(L+1)r} \rangle = \frac{1}{2} r K [N + 1 - r] \quad (16)$$

Due to the modified hopping rates in the neighborhood of the intersections the density profile is linear between $\langle n_{(L+1)r-1} \rangle$ and $\langle n_{(L+1)r-L} \rangle$ rather than between the intersections ρ_r and ρ_{r-1} itself. This becomes noticeable for large reservoir densities ρ . There is a "jump" between intersections and their adjacent lattice sites. Fig. 11 illustrates this by means of a profile obtained from MC simulations). Let us consider a channel segment embedded by the two intersections ρ_r and ρ_{r-1} . Solving (13) for the lattice sites located next to the intersections leads to

$$\langle n_{(L+1)r-1} \rangle = \frac{\rho_{r-1} + \rho_r (L - (L-1)\rho)}{(L+1) - 2L\rho + (L-1)\rho^2} \quad (17)$$

$$\langle n_{(L+1)r-L} \rangle = \frac{\rho_r + \rho_{r-1} (L - (L-1)\rho)}{(L+1) - 2L\rho + (L-1)\rho^2} \quad (18)$$

and for the very first channel segment we find

$$\langle n_L \rangle = \frac{L\rho_1}{L+1 - L\rho}. \quad (19)$$

We have now fully determined the profile for MTC systems with small reactivity. The currents between neighboring lattice sites are proportional to the density difference $j_{(x,x+1)} \sim (\langle n_{x+1} \rangle - \langle n_x \rangle)$ with a proportional constant being the actual hopping rate.

Fig. 12 shows the simulated profile of a β channel together with the theoretical densities. We chose an intermediate reservoir density $\rho = 0.5$. The collapse of the two curves is very good. In order to study the quality of the approximation for different sets of parameter we use the definition (12) above. The normalized mean square deviation Q is plotted for different L and different ρ (Fig. 13). In the regime of interest, i.e. for small reactivities, the profile is well described by the theory even for small L and rather high reservoir densities.

VI. CONCLUSION

Our simulations and analytical results describe the MTC effect quantitatively over a wide range of parameters within the NBK model. Moreover, trends which are independent

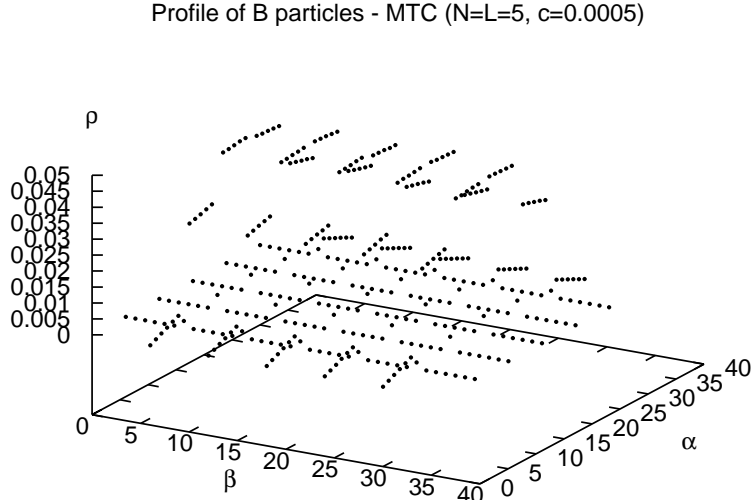


FIG. 11: Demonstration of "jumps" at intersections for large ρ . Here we choose $\rho = 0.9$.

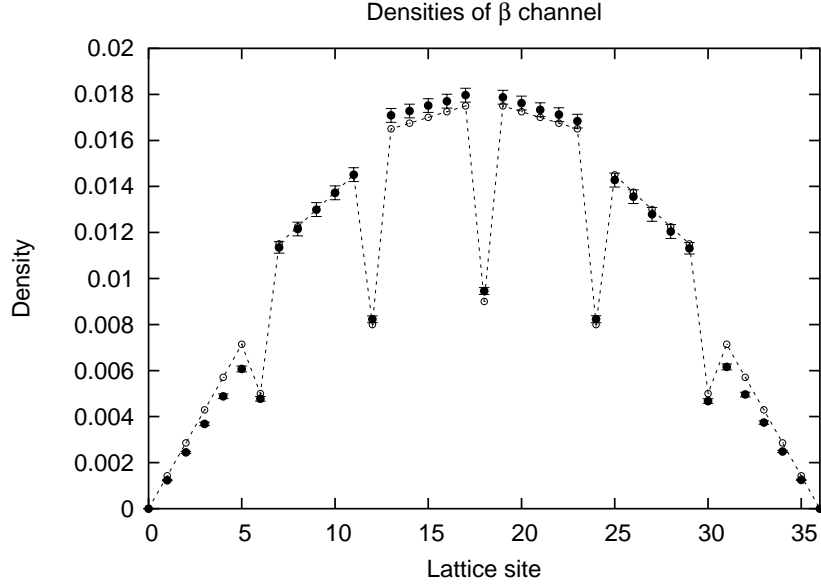


FIG. 12: Densities of a β channel. Small open circles connected with the dotted line show the theoretical densities. Solid circles are densities obtained by MC simulation ($N = L = 5$, $c = 0.0005$, $\rho = 0.5$) .

of model details have been identified by analytical calculations and lead to a more positive result than concluded by [12] where no MTC effect at all was reported for short interconnecting channels $L = 1$. For reasonable reactivities and channel lengths the MTC effect vanishes proportionally to $1/N$, i.e., is inversely proportional to the grain diameter. This

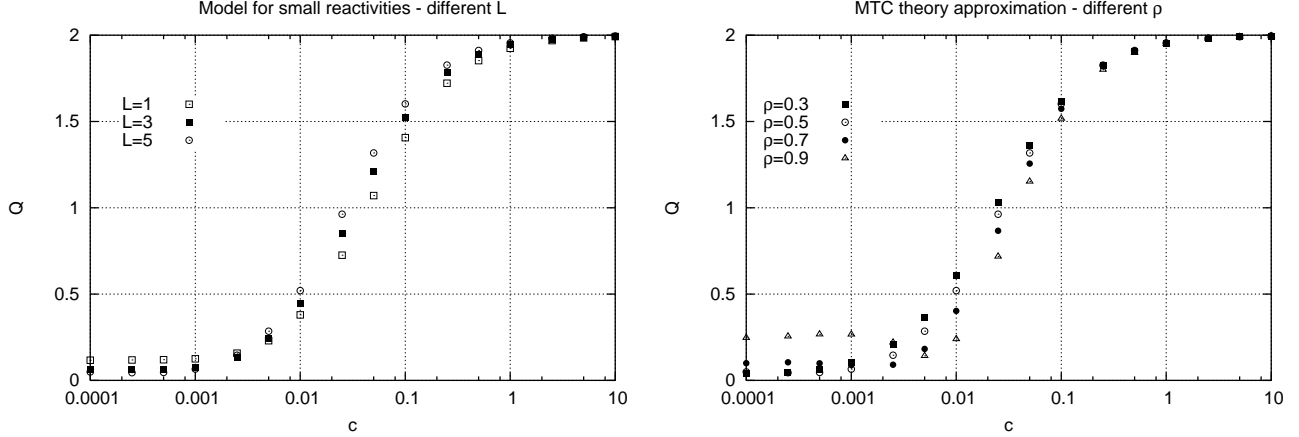


FIG. 13: Collapse of the simulated and calculated profiles for MTC systems. Left: $N = 5$, $\rho = 0.5$ and different L . Right: $N = 5$, $L = 5$ and different ρ .

was shown explicitly for a two-dimensional simulation model, but the reasoning that led to this conclusion extends straightforwardly to a three-dimensional system. Nevertheless, for optimized external process parameters the NBK model exhibits an enhancement of the effective reactivity of up to approx. 30% for small grains and any (even short) channel length and reactivity c . In the present study we have not taken into consideration that smaller molecules may diffuse into larger channels, not only the smaller channels. This was done in order to keep the model simple so that the origin of the observed MTC effect becomes as transparent as possible. We did make simulations for a different model where this mechanism is taken into account. We have found in these simulations that the MTC effect becomes stronger. In summary, our investigations suggest that MTC may enhance significantly the effective reactivity in zeolitic nanoparticles with suitable binary channel systems and thus may be of practical relevance in applications.

-
- [1] Ch. Baerlocher, W. M. Meier and D. H. Olson, Atlas of Zeolite Structure Types, Elsevier: London 2001.
 - [2] J. Kärger and D.M. Ruthven, Diffusion in Zeolites and Other Microporous Solids, Wiley: New York 1992.
 - [3] E.G. Derouane and Z. Gabelica, J. Catal. 65 (1980) 486.
 - [4] E.G. Derouane, Appl. Catal. A, N2 (1994) 115.

- [5] R. Q. Snurr and J. Kärger, Phys. Chem. B 101 (1997) 6469.
- [6] L. A. Clark, G. T. Ye, R. Q. Snurr, Phys. Rev. Lett. 84 (2000) 2893.
- [7] L. A. Clark, G. T. Ye, A. Gupta, L. L. Hall, R. Q. Snurr, J. Chem. Phys. 111 (1999) 1209.
- [8] M. Heuchel, R. Q. Snurr, E. Buss, Langmuir 13 (1997) 6249.
- [9] N. Neugebauer, P. Bräuer, J. Kärger, J. Catal. 194 (2000) 1.
- [10] J. Kärger, P. Bräuer, H. Pfeifer, Z. Phys. Chem. 104 (2000) 1707.
- [11] J. Kärger, P. Bräuer, A. Neugebauer, Europhys. Lett. 53 (2001) 8.
- [12] P. Bräuer, A. Brzank, J. Kärger, J. Phys. Chem. B 107 (2003) 1821.
- [13] A. Brzank, G. M. Schütz, P. Bräuer, and J. Kärger, Phys. Rev. E 69 (2004) 031102.
- [14] J.S. Beck, J.C. Vartulli, W.J. Roth, M.E. Leonowice, C.T. Kresge, K.D. Schmitt, C. T-W. Chu, D.H. Olsen, E.W. Sheppard, S.B. McCullen, J.B. Higgins, J.L. Schlenker, J. Am. Chem. Soc. 114 (1992) 10834.
- [15] J.H. Sun, Z. Shan, Th. Maschmeyer, M.-O. Coppens, Langmuir 19 (2003) 8395.
- [16] F. Spitzer, Adv. Math. 5 (1970) 246.
- [17] H. Spohn, J. Phys. A 16 (1983) 4275.
- [18] H. van Beijeren, K.W. Kehr, R. Kutner, Phys. Rev. B 28 (1983) 5711.
- [19] G. Schütz, S. Sandow, Phys. Rev. E 49 (1994) 2726.
- [20] T.M. Liggett: *Stochastic Interacting Systems: Contact, Voter and Exclusion Processes* (Springer, Berlin, 1999).
- [21] G.M. Schütz, in: *Phase Transitions and Critical Phenomena*, C. Domb and J. Lebowitz (eds.), (Academic, London, 2001).
- [22] C. Rödenbeck, J. Kärger, J. Chem. Phys. 110 (1999) 3970.